Angle-resolved photoemission spectroscopy of $Sr_2CuO_2Cl_2$

C. Dürr, S. Legner, R. Hayn, S. V. Borisenko, Z. Hu, A. Theresiak, M. Knupfer, M. S. Golden, and J. Fink
Institute for Solid State and Materials Research Dresden, P.O. Box 270016, D-01171 Dresden, Germany

F. Ronning and Z.-X. Shen
Department of Physics and Stanford Synchrotron Radiation Laboratory, Stanford University, Stanford, California 94305-4045

H. Eisaki and S. Uchida
Department of Superconductivity, The University of Tokyo, Bunkyo-ku, Tokyo 113, Japan

C. Janowitz and R. Müller
Institut für Physik der Humboldt-Universität Berlin, Invalidenstrasse 110, 10115 Berlin, Germany

R. L. Johnson
II. Institut für Experimentalphysik der Universität Hamburg, Luruper Chaussee 149, 22761 Hamburg, Germany

K. Rossnagel and L. Kipp
Institut für Experimentelle und Angewandte Physik, Christian-Albrechts-Universität zu Kiel, Leibnizstrasse 19, 24118 Kiel, Germany

G. Reichardt
BESSY GmbH, Albert-Einstein-Strasse 15, 12489 Berlin, Germany

We have investigated the lowest binding-energy electronic structure of the model cuprate $Sr_2CuO_2Cl_2$ using angle-resolved photoemission spectroscopy. Our data from about 80 cleavages of $Sr_2CuO_2Cl_2$ single crystals give a comprehensive, self-consistent picture of the nature of the first electron-removal state in this model undoped CuO_2-plane cuprate. First, we show a strong dependence on the polarization of the excitation light which is understandable in the context of the matrix element governing the photoemission process, which gives a state with the symmetry of a Zhang-Rice singlet. Secondly, the strong, oscillatory dependence of the intensity of the Zhang-Rice singlet on the exciting photon energy is shown to be consistent with interference effects connected with the periodicity of the crystal structure in the crystallographic c direction. Thirdly, we measured the dispersion of the first electron-removal states along $\Gamma \rightarrow (\pi,\pi)$ and $\Gamma \rightarrow (\pi,0)$, the latter being controversial in the literature, and have shown that the data are best fitted using an extended tJ model, and extract the relevant model parameters. An analysis of the spectral weight of the first ionization states for different excitation energies within the approach used by Leung *et al.* [Phys. Rev. B **56**, 6320 (1997)] results in a strongly photon-energy dependent ratio between the coherent and incoherent spectral weight. The possible reasons for this observation and its physical implications are discussed.

I. INTRODUCTION

Extensive effort continues to be expended to understand the electronic properties of the cuprate high-T_c superconducting compounds. Apart from many differences, the cuprate superconducting materials have important properties in common. Namely, they are all layered compounds possessing CuO_2 planes, where the origin of the superconducting behavior is to be found. The electronic structure of the states with the lowest binding energy is satisfactorily understandable only in models which take into account correlation effects. Angle-resolved photoemission spectroscopy (ARPES) has proven to be a powerful tool to investigate the low binding-energy electronic structure of the cuprates. Important examples for the success of this method are the mapping of the Fermi surface[1] and the determination of an anisotropy of the superconducting gap consistent with a d-wave order parameter.[2]

In the undoped regime the cuprates are two-dimensional antiferromagnetic insulators with CuO_2 planes resulting in a correlation-gapped half-filled $Cu3d_{x^2-y^2}$-$O2p_x$/$O2p_y$ antibonding band of lowest binding energy. Upon doping with holes, the states with lowest binding energy evolve towards the chemical potential, and the cuprate becomes metallic or superconducting. To clarify the main principles of the evolution of the lowest binding-energy states with doping by applying model Hamiltonians, one has to go step by step from simple situations or limiting cases to more complicated scenarios. A natural starting point, then, is to investigate the propagation of a single hole in a CuO_2 plane by studying the undoped parent compounds of cuprate superconductors by photoemission, where one electron is removed from the CuO_2 plane. The states thus investigated can be termed the first electron-removal states.

A special class of parent compounds are the oxyhalides such as $Sr_2CuO_2Cl_2$, $Ca_2CuO_2Cl_2$, $Sr_2CuO_2F_2$ (one layer
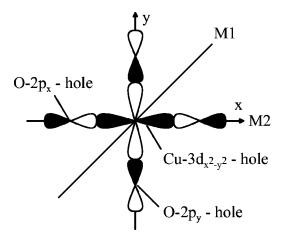
FIG. 1. Schematic representation of the Zhang-Rice singlet state in the one-particle representation. The Zhang-Rice singlet has the same symmetry as a $d_{x^2-y^2}$ orbital, implying the existence of two mirror planes perpendicular to the CuO$_2$-plane, labeled M_1 and M_2.

compounds), and Ca$_3$Cu$_2$O$_4$Cl$_2$ (double layered compound),[3,4] all of which contain an apical halogen atom, rather than an oxygen. It is now well established that the apical oxygen which is contained in most of the cuprate superconductors is not necessary for high-T_c superconductivity as Hiroi *et al.*[5] showed that Ca$_{2-x}$Na$_x$CuO$_2$Cl$_2$ is superconducting ($T_c = 26$ K). Out of the class of cuprate parent compounds without apical oxygen, the layer compound Sr$_2$CuO$_2$Cl$_2$ is remarkable due to its extremely stable stoichiometry. Despite considerable efforts so far it has not been possible to dope this substance chemically. Furthermore, the CuO$_2$ planes are unbuckled and the crystal structure shows neither orthorhombic distortion nor a superstructure at least down to 10 K (Ref. 6). Therefore, Sr$_2$CuO$_2$Cl$_2$ can be seen as the best realization of a two-dimensional antiferromagnet at half-filling and it is in this limit an ideal test case for any Hamiltonian in the low-doping regime.

In theoretical studies, the lowest binding-energy ionization states of the cuprates were predicted to be essentially described by a singlet antibonding combination of a Cu3$d_{x^2-y^2}$ orbital [containing the intrinsic Cu3d (Ref. 9) hole] and a coherent combination of the four neighboring O2p_x/O2p_y orbitals which can be thought of as containing the hole created in the photoemission process.[7,8] This two-hole state is generally referred to as the Zhang-Rice singlet state.[9] The singlet character of the first electron-removal states, at least in CuO, has been experimentally verified using spin-resolved resonant photoemission.[10]

There are various possibilities to theoretically model the dynamics of this lowest binding-energy excitation. For instance, in the framework of a three-band Hubbard Hamiltonian (H_{3b}), the Zhang-Rice singlet state is a two-particle state and belongs to the A_{1g} (totally symmetric) irreducible representation of the eigenstates of H_{3b}. In the one-band Hubbard Hamiltonian (H_{1b}), the tJ model and its extensions, the Zhang-Rice singlet state is an one-particle state belonging to the B_{1g} irreducible representation and has the same symmetry as a Cu3$d_{x^2-y^2}$ orbital. Figure 1 shows a schematic representation of a Zhang-Rice singlet state, in-

cluding the two mirror planes M_1 and M_2 which are perpendicular to the CuO$_2$ plane and which are relevant for photoemission along $\Gamma \rightarrow (\pi,\pi)$ and $\Gamma \rightarrow (\pi,0)$, respectively.

It is now generally accepted that the H_{3b} is a good starting point to describe the low binding-energy electronic structure in the strongly correlated cuprate systems and consequently the H_{3b} has been investigated in detail.[11] Additionally, it has been shown that the H_{1b} still carries enough information to describe the low-energy dynamics in the cuprates.[12] In the next level of simplifying these models, the Hubbard Hamiltonian can be expressed in terms of new Fermionic operators. In the large-U-limit, this new Hamiltonian can be written in a t^2/U series and gives an effective one-band Hamiltonian, the tJ model. This has been shown to give the same results for both the H_{3b} (Ref. 7) and the H_{1b} (Ref. 13) approaches. Extensions of the tJ model have been carried out mainly in two different ways. First, two further parameters — t' describing the diagonal hopping and t'' for the next nearest neighbor hopping — can be introduced in addition to the direct hopping t.

The fact that a t-mediated hopping creates strings of spin defects leads to a predicted bandwidth for the Zhang-Rice singlet state which is governed by $t^2/U \sim J$. Hopping events mediated by t' and t'', however, take place on the same spin sublattice and therefore even taking small values of these parameters has a significant effect on the results the tJ model gives for the **k**-dependent spectral function of the Zhang-Rice singlet state. Secondly, the tJ model has also been extended to take three-site hopping terms (proportional to $J/4$) into account,[14] which appear in a natural way if one employs a more detailed derivation of an effective Hamiltonian for the low binding-energy excitations.[15]

A different ansatz to understand the dynamics of holes in CuO$_2$ planes was proposed by Laughlin.[16] He argued that the hole created by photoemission decays into spin and charge degrees of freedom and that the photoemission experiment measures the dispersion of the spinon.[16] However, in a gauge-field treatment of this model this decay of the quasiparticles is suppressed below the Néel temperature, T_N, due to confinement.[17] Another fundamental approach to calculate the properties of the Hubbard Hamiltonian and the tJ models uses the fact that they share an approximate SO(5) symmetry.[18]

The preceding discussion highlights the intense theoretical interest in the lowest binding-energy electron-removal states of the undoped cuprates. Although originally trailing a few years behind the theoretical work, experimental investigations of the first electron-removal state in undoped cuprates have been carried out using ARPES.[19–23] Before going on to mention the status in the field to date, we first ask the question: what kind of information does an ARPES experiment provide us with?

Neglecting ''extrinsic'' effects such as scattering of the photoelectrons on their way to the surface and assuming the applicability of the sudden approximation, the photoemission intensity $I(\mathbf{k},E)$, reads

$$I(\mathbf{k},E) \sim \sum_{|i\rangle,|f\rangle} |M_{i,f}|^2 S(\mathbf{k},E) f(E), \qquad (1)$$

where the sum runs over all final states and initial states, $f(E)$ denotes the Fermi function and $S(\mathbf{k},E)$ the spectral function:

$$S(\mathbf{k},E) = -\frac{1}{\pi} \mathrm{Im} \langle i|c_{\mathbf{k}} \frac{1}{E-H+E_i} c_{\mathbf{k}}^{\dagger}|i\rangle. \qquad (2)$$

$M_{i,f} = \langle f|\mathbf{A}\cdot\mathbf{p}|i\rangle$ is the matrix element to be taken between the initial state $|i\rangle$ with energy E_i and final states $|f\rangle$ with energy E, $\mathbf{A}\cdot\mathbf{p}$ is the photoemission interaction operator and H the Hamiltonian of the system. From an ARPES experiment one can gain mainly two kinds of information. First, the spectral function $S(\mathbf{k},E)$ gives direct information about the dispersion and the quasiparticle character of the states and can be compared directly to predictions of model Hamiltonians. All information carried by $S(\mathbf{k},E)$ is expected to be *independent* of the excitation energy and geometry of the experiment. Secondly, the matrix element $M_{i,f}$ includes all information concerning the photoemission interaction. As such it is sensitive to the experimental geometry via symmetry selection rules as well as to the photon energy.

The first ARPES experiments on $Sr_2CuO_2Cl_2$ (Ref. 19) were able to make the important observation that the Zhang-Rice singlet state bandwidth along $\Gamma \rightarrow (\pi,\pi)$ is of the order of $2J$, and that the Zhang-Rice singlet state approaches closest to the chemical potential at the $(\pi/2,\pi/2)$ point. These observations fit the predictions of the tJ-model. However, these early experiments found very little dispersion along $\Gamma \rightarrow (\pi,0)$, which is in conflict with the predictions of the same model. Subsequent studies have confirmed the behavior along $\Gamma \rightarrow (\pi,\pi)$, but have also observed dispersion along the $\Gamma \rightarrow (\pi,0)$ direction in reciprocal space (**k** space).[20,21,23]

Nevertheless, the situation as regards the exact dispersion relation along $\Gamma \rightarrow (\pi,0)$, and in particular concerning the minimum energy difference between the states along $\Gamma \rightarrow (\pi,0)$ and those at the $(\pi/2,\pi/2)$ point is unclear. This is more than a mere ARPES detail, as it is along the $\Gamma \rightarrow (\pi,0)$ direction that the predictions of the different models vary the most — thus making this direction in **k** space important for the quantitative comparison between theory and experiment.

Furthermore, the recent controversy surrounding the correct Fermi surface topology in the doped high temperature superconductor $Bi_2Sr_2CaCu_2O_{8+\delta}$ (Ref. 24) has illustrated that data sets recorded from the same system with different experimental conditions can be remarkably dissimilar. Consequently, both the photon energy and exact polarization geometry used in an ARPES experiment are important parameters which, if they cannot be treated at a quantitative, microscopic level, should at least be thoroughly investigated on the experimental side.

In this paper, we address the electronic structure and dynamics of the lowest binding-energy electron-removal states in the ''standard'' undoped model cuprate $Sr_2CuO_2Cl_2$ using ARPES. Following the description of the experimental status given above, our ''re-visit'' of this system concentrates on the following points.

(a) A thorough characterization of the photon-energy dependence of the first electron-removal states at $(\pi/2,\pi/2)$ and close to $(\pi/2,0)$ [the two points along $\Gamma \rightarrow (\pi,\pi)$ and $\Gamma \rightarrow (\pi,0)$ for which the first electron-removal states have maximum spectral weight]; (b) a thorough characterization of the polarization dependence of the first electron-removal states along these high-symmetry directions in **k** space; (c) the determination of the dispersion relation of the first electron-removal states along $\Gamma \rightarrow (\pi,\pi)$ and $\Gamma \rightarrow (\pi,0)$, with subsequent comparison of the results with both existing ARPES data and the predictions of an extended tJ model and; (d) the determination of the **k**-dependent evolution of the coherent and incoherent parts of the spectral weight of the first electron-removal state along $\Gamma \rightarrow (\pi,\pi)$ and $\Gamma \rightarrow (\pi,0)$, and comparison of these data with theoretical predictions.

II. EXPERIMENT

Experiments were performed at the beamlines F2.2 and W3.2 at the Hamburg Synchrotron Laboratory (HASYLAB), at the undulator beamline U2-FSGM and the 2m SEYA beamline at the Berliner Elektronenspeicherring Gesellschaft für Synchrotronstrahlung mbH (BESSY). At the storage rings and monochromators used in these studies, highly linearly polarized synchrotron radiation was available. In addition, the crossed undulator U2-FSGM beamline gave the possibility to use vertically oriented linearly polarized light. At this latter facility, polarization-dependent measurements could be performed without changing any other parameter in the experiment. A total energy resolution (beamline and analyzer) of better than 70 meV and an angular acceptance of the analyzer of $\pm 1°$ was used. Fresh samples of $Sr_2CuO_2Cl_2$ were cleaved *in situ* at a base pressure of 1×10^{-10} mbar, and spectra were taken within six hours after cleavage. Samples were either preoriented using x-ray diffraction measurements or aligned *in situ* with the aid of low energy electron diffraction (LEED). In all cases, the fine angular adjustment was carried out using the **k**-space symmetry of the sharp ARPES features related to nonbonding $O2p$ states around (π,π) and $(\pi,0)$, as discussed in Refs. 25 and 26.

The high-quality single crystalline $Sr_2CuO_2Cl_2$ was grown according to the method described in Ref. 3, where predried high-purity $SrCO_3$, $SrCl_2$, and CuO in a ratio 1:1:1 were melted at 1100°C. Although T_N for $Sr_2CuO_2Cl_2$ is 251 K (Ref. 6), all ARPES experiments were carried out at room temperature. This decision was based on two arguments. First, and most importantly, as these experiments involve electron ejection from perfect single crystals of a compound with an energy gap of the order of 2 eV, we had to eliminate uncertainties due to charging effects, which meant measuring at room temperature. Secondly, although we measure at a temperature some 50 K above the Néel temperature, it has been shown that the antiferromagnetic spin correlation length of $Sr_2CuO_2Cl_2$ at 350 K is still 250 Å (Ref. 27), meaning that the lowest binding-energy hole state created in the photoemission process is still embedded in an antiferromagnetic spin background.

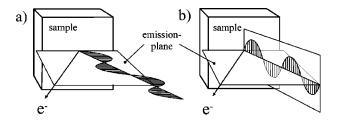To be absolutely sure that variations in the flux of the

FIG. 2. The experimental geometry for the photoemission experiments: (a) emission plane and polarization plane are parallel to each other; (b) emission plane and polarization plane are perpendicular to each other. Throughout this paper we call the first case (a) *parallel* and the second case (b) *perpendicular* polarization.

incident photons from the storage ring did not lead to charging-induced energy shifts, we also adjusted the beamline such that the photon flux impinging on the sample (monitored with a gold mesh upstream of the sample) was constant. This means that measuring time is the only parameter required for the normalization of the data. Bearing in mind that the data presented here are a selection of data from about 80 different cleavages, we made the qualitative observation that best and sharpest energy distribution curves (EDC) were observed for samples which behaved most sensitively to charging effects. This relation, of course, is reasonable as it correlates cleavage quality with the intrinsically highly insulating nature of perfect $Sr_2CuO_2Cl_2$.

Essentially two different experimental geometries were used. They can be characterized by the orientation of two planes: (a) the plane of polarization and (b) the emission plane. The plane of polarization is the plane spanned by the vector of the direction of the synchrotron light and the vector of its electric field (vector of polarization). The emission plane includes the vector of the direction of the photoelectron and the surface normal. Throughout this paper we call the experimental geometry *parallel* if these two planes are parallel, *perpendicular* if these two planes are perpendicular to each other (see Fig. 2 for a sketch of the two geometries).

III. PHOTON-ENERGY AND POLARIZATION DEPENDENCE OF THE FIRST ELECTRON-REMOVAL STATES OF AN UNDOPED CuO₂ PLANE

As mentioned above, both the inconsistencies in the literature regarding the dispersion relation of the first electron-removal states along the $\Gamma \rightarrow (\pi,0)$ direction (Ref. 28) in $Sr_2CuO_2Cl_2$, as well as the ongoing controversy regarding the photon-energy dependence of the ARPES data from $Bi_2Sr_2CaCu_2O_{8+\delta}$, mean that before comparison with theory is carried out, the photon-energy dependence of the first electron-removal states should be examined in detail.

In Fig. 3, photon-energy dependent ARPES data for the first electron-removal state in $Sr_2CuO_2Cl_2$ at two points in the Brillouin zone: (a) $(\pi/2,\pi/2)$ (perpendicular geometry) and (b) $(0.7\pi,0)$ (parallel geometry) are shown. In these regions of **k** space the spectral weight of the first electron-removal state is known to be at a local maximum along the respective **k**-space directions.[19–21,23] The spectra, which are normalized as described in the last section, illustrate clearly
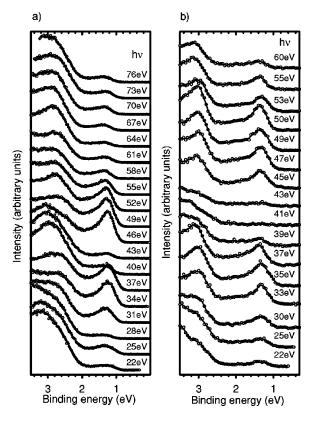

FIG. 3. A typical example of ARPES data of the first electron-removal states of $Sr_2CuO_2Cl_2$ as a function of photon energy. In panel (a) the ARPES EDC's are recorded at $(\pi/2,\pi/2)$ and in panel (b) at $(0.7\pi,0)$. The photon energies are as shown.

the strong variation of the first electron-removal state intensity with photon energy. The data shown in Fig. 3 represent only a small portion of the photon-energy dependent data recorded, and are intended to give the reader a direct impression of the strength of the effects at play. Each of the shown spectra is part of a short $k_\parallel$ series of three or five spectra. This was done to ensure we always captured the spectrum with the highest spectral intensity for the first electron-removal states. Within the errors given by the finite **k** resolution of the experimental setup (0.054 Å⁻¹ for 16 eV photon-energy up to 0.152 Å⁻¹ for 80 eV photon-energy) we found the highest intensities always at the same **k** positions, namely at $(\pi/2,\pi/2)$ and at $(0.7\pi,0)$.

This is in contrast to the results reported in Ref. 23, where series of EDCs on $Sr_2CuO_2Cl_2$ along $\Gamma \rightarrow (\pi,\pi)$ taken with two different photon-energies show differences not only in intensity, but also in the EDC-derived dispersion relation of the first ionization states. This was discussed in Ref. 23 as *not* being due to either (a) the experimental setup, (b) the excitation of different initial states, or (c) in the variation of $k_\perp$ of the photoelectron. The effect was rather attributed to the strong impact of the matrix element, not only on the strength of the photoemission signal but also on the position of the quasiparticle peak in the photoemission spectra, leading to differences in the EDC-derived dispersion relations. We are forced to disagree with the last point, as in our extensive collection of ARPES data, there was never evidence for a photon-energy dependent shift of the **k** position for
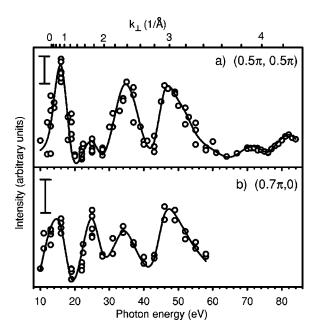
FIG. 4. The photon-energy dependence of the photoemission intensity of the first electron-removal states (a) at $(\pi/2,\pi/2)$ and (b) at $(0.7\pi,0)$, arrived at from the analysis of a large body of ARPES data such as that shown in Fig. 3. The solid black line represents a guide to the eye and the error bars (located in the upper left corner of each panel) indicate the error of the fit to the experimental intensity (95% confidence interval). The top axis shows the corresponding $k_\perp$ scale calculated using an inner potential of 8.0 eV (for details see text).

which the first electron-removal states have minimum binding energy along $\Gamma\rightarrow(\pi,\pi)$. The same, in fact, holds for other directions in the Brillouin zone as well as for the dispersion of other features with low binding energy. If matrix element effects change the EDC-derived dispersion relation, then this change is, at least for our data, smaller than the energy resolution and angular resolving power of our ARPES experiments, which is equal to Δ_k or better than Δ_E the values used in Ref. 23.

Figure 4 shows an analysis of the spectral weight of the first electron-removal states at the same **k** points as shown in Fig. 3. These data are derived from a large set of photon-energy dependent ARPES data covering measurements from 10 (6) cleaves for the upper (lower) panels. From Fig. 4 it is clear that the ARPES spectral weight of the first electron-removal states oscillates with the final state kinetic energy, that is with $k_\perp$. We used a value of 8.0 eV for the inner potential E_0 ($E_0 = V_0 - \Phi$, where Φ is the work function) to calculate $k_\perp$, a value which in the range of $6.9-8.9$ eV used by other groups.[29] We see clear maxima at $k_\perp = 0.82$, 1.63, 2.40, and 3.12 Å^{-1}, corresponding to photon energies of 16, 25, 35, and 48 eV.

The oscillatory nature of the photon-energy dependence, coupled to the absence of a classical resonance behavior at the Cu $3p$ threshold (around 74–76 eV photon energy) indicates that the factor dominating the observed behavior is something other than the atomic photoionization cross sections, and could be related, for example, to the extreme two-dimensionality of the electronic states concerned. This could

lead to a matching of the final state $k_\perp$ to the periodicity of the unit cell of $Sr_2CuO_2Cl_2$ in c direction. Note that the differences between the four $k_\perp$ is $0.72-0.81$ Å^{-1} which represents in real space a distance of $7.8-8.7$ Å which is comparable to c-axis separation of two neighboring CuO_2 planes $(=7.805$ Å$)$ in $Sr_2CuO_2Cl_2$. The oscillation of the photoemission intensity with photon-energy can therefore be attributed to interference effects of the photoelectron wave diffracted from the c-axis periodicity of the layered crystal structure, similar to the explanation of the strong photon energy dependence of the photoemission intensity from the molecular orbitals of C_{60} (Ref. 30).

These strong variations in intensity as a function of photon-energy are also reminiscent of ARPES data of $YBa_2Cu_3O_{7-\delta}$, in which an out-of-phase behavior regarding intensity vs $k_\perp$ was observed for the CuO_2-derived band which crosses the Fermi energy near the $\bar{X}$ point and the so-called "1 eV peak."[31] This fact was, at that time, used to argue against the surface-state origin of the 1 eV peak, a feature which is now believed to be due to nonmixing O2p states of particular symmetry.[25] Nevertheless, the data presented here, taken together with the theoretical and experimental investigations on $Bi_2Sr_2CaCu_2O_{8+\delta}$ (Refs. 32 and 24), indicate clearly that care should be taken in the interpretation of absolute spectral weights observed in the ARPES data of the layered cuprates, as matrix element and diffraction effects do play an important role in these systems.

A further experimental variable in an ARPES experiment is the polarization of the incoming radiation. Figure 5 shows two series of ARPES measurements on $Sr_2CuO_2Cl_2$ recorded along the high-symmetry directions $\Gamma\rightarrow(\pi,0)$ and $\Gamma\rightarrow(\pi,\pi)$. The photon-energy was set to 22.4 eV, which is near a maximum of intensity as shown in Fig. 3 above. In each case, the series are presented in pairs of data sets recorded with perpendicular and parallel polarization geometries as described in the experimental section.

Along the $\Gamma\rightarrow(\pi,\pi)$ direction in **k** space the first electron-removal state feature shows highest photoemission intensity with perpendicular geometry [Fig. 5(a)], whereas along $\Gamma\rightarrow(\pi,0)$ maximal intensities are observed in the parallel geometry [Fig. 5(d)], a result which tallies with earlier measurements with 25 eV photon energy.[20] This remarkable dependence of the photoemission intensity on the polarization was first explained in the context of the strong polarization dependence in photoemission data from surface states.[33]

The physical picture behind the polarization dependence can be described as follows. The interaction operator $\mathbf{A}\cdot\mathbf{p}$ has even $(+)$ parity in a *parallel* and odd $(-)$ parity in a *perpendicular* experimental geometry. Assuming the applicability of the Zhang-Rice singlet state construction to the first electron-removal final state, in a many-body picture this state belongs to the A_{1g} representation, therefore being totally symmetric. Thus in this representation the Zhang-Rice singlet has even parity with respect to a mirror plane along the Cu3$d_{x^2-y^2}$-O2p_x/O2p_y orbital bonds (M_2) as well as at 45° to the bonds (M_1). In **k** space M_1 corresponds to the $\Gamma\rightarrow(\pi,\pi)$ direction and M_2 to $\Gamma\rightarrow(\pi,0)$. The initial state
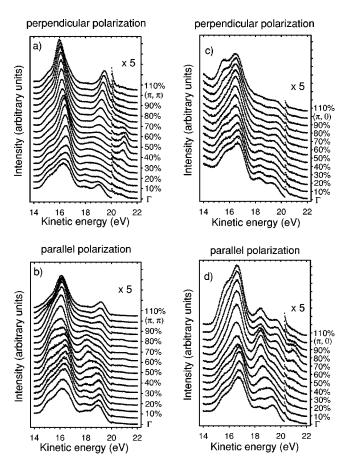
FIG. 5. Series of energy-distribution curves for different polarization geometries. The photon energy was set to 22.4 eV and all spectra were taken at 300 K. Panels (a) and (b) show measurements along $\Gamma \to (\pi,\pi)$ where the first electron-removal state peak appears near 21.0 eV kinetic energy for perpendicular polarization in (a). The corresponding series along $\Gamma \to (\pi,0)$ are shown in panels (c) and (d). There, the first electron-removal states gives significant photocurrent near 20.9 eV kinetic energy only for parallel polarization in (d).

(ground state) is a one-hole state with $d_{x^2-y^2}$ symmetry, and therefore has even parity with respect to M_2 and odd parity with respect to M_1. The matrix element thus formally vanishes for the two cases

$$\text{parallel for } \Gamma \to (\pi,\pi) \Rightarrow M \sim \langle + | + | - \rangle = 0,$$

$$\text{perpendicular for } \Gamma \to (\pi,0) \Rightarrow M \sim \langle + | - | + \rangle = 0.$$

This argumentation also holds in the one band picture. Here the initial state (ground state) is totally symmetric and the final state has $d_{x^2-y^2}$ symmetry (as shown in Fig. 1), leading to the same result.

Thus the observed polarization dependence of the first electron-removal states of an undoped CuO$_2$ plane indicates that these states have a symmetry fully consistent with that of the Zhang-Rice singlet. These results amend earlier reports (Ref. 26) regarding the polarization dependence of the first electron-removal states along $\Gamma \to (\pi,0)$ in Sr$_2$CuO$_2$Cl$_2$.

IV. THE DISPERSION RELATION AND SPECTRAL FUNCTION OF THE FIRST ELECTRON-REMOVAL STATES

The common picture given by the tJ model and its extensions[34–37] is a strong dispersion of the Zhang-Rice singlet state along the $\Gamma \to (\pi,\pi)$ direction with the minimum binding energy at $(\pi/2,\pi/2)$. At this **k** point, the spectral weight of the first electron-removal state also has its maximum and vanishes going away from $(\pi/2,\pi/2)$. Recent ARPES experiments on Sr$_2$CuO$_2$Cl$_2$ confirm this.[19–21,23,25] Along the $\Gamma \to (\pi,0)$ direction the tJ model predicts a rather low binding energy near the high-symmetry point $(\pi,0)$ which is, in fact, almost energetically degenerate with that at $(\pi/2,\pi/2)$. In the same model, the spectral weight of the quasiparticle increases and is maximal at $(\pi,0)$. This is in contrast to the result given in Ref. 19 where no dispersion was observed and in Refs. 20,21,23 where the binding energy of the first electron-removal state increases and the quasiparticle weight decreases after $(\pi/2,0)$. For the $(\pi,0) \to (0,\pi)$ direction, the tJ model predicts only little dispersion, whereas experiment has shown a strong isotropic dispersion around the $(\pi/2,\pi/2)$ point (Ref. 19). Extensions of the tJ model and the spin and charge separation ansatz exhibit new properties along $\Gamma \to (\pi,0)$ and $(\pi,0) \to (0,\pi)$. The Zhang-Rice singlet state around $(\pi,0)$ can now lower its energy by delocalization and is thus pushed to higher binding energies and the dispersion in this direction is essentially parabolic. In these models, both a quasiparticle dispersion along $(\pi,0) \to (0,\pi)$ which is isotropic around $(\pi/2,\pi/2)$ as well as a reduced spectral weight near $(\pi,0)$ can be achieved. In the spin and charge separation model the isotropy along $\Gamma \to (\pi,\pi)$ and $(\pi,0) \to (0,\pi)$ is intrinsic and near $(\pi/2,\pi/2)$ the dispersion relation is wedge-like rather than parabolic. Surprisingly, the data in Ref. 19 agree well with the extended tJ model along $(\pi,0) \to (0,\pi)$, but not along $\Gamma \to (\pi,\pi)$. In contradiction to that, other data along $\Gamma \to (\pi,0)$ are consistent with the extended tJ model and the spin and charge ansatz,[20] a view which appears to be supported by further data sets.[21,23] Thus, the experimental dispersion along the $\Gamma \to (\pi,0)$ remains controversial, and yet it is the dispersion and the evolution of the spectral weight along $\Gamma \to (\pi,0)$ that is of the deepest theoretical interest for the following reasons. First, the states near $(\pi,0)$ evolve with increasing hole concentration to become the flat bands located near the chemical potential in the metallic systems. These flat band regions are believed by some to hold the key to high temperature superconductivity. Secondly, the dispersion and quasiparticle spectral weight along $\Gamma \to (\pi,0)$ are fingerprints for the different models and parameters used in them. Thirdly, there are strong indications that the dispersion in the insulator is closely connected with the pseudogap in the underdoped region of the high-T_c superconductor phase diagram and thus may also be related to the superconducting gap in the doped superconducting systems.[17,22]

Consequently, the importance of experimental data which allow the determination of the dispersion and spectral weight of the first electron-removal states along $\Gamma \to (\pi,0)$ cannot
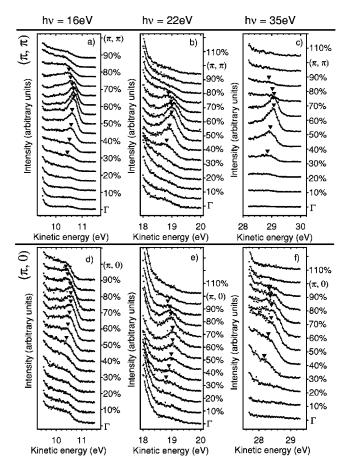
FIG. 6. ARPES series showing the dispersion of the Zhang-Rice singlet state along the high-symmetry directions. The upper three panels show series along $\Gamma \rightarrow (\pi,\pi)$ the lower three panels along $\Gamma \rightarrow (\pi,0)$. The excitation energy is the same for each column, 16 eV (left), 22 eV (center), and 35 eV (right). Black triangles are included as a guide indicating the kinetic energy of the first ionization state determined by a fitting procedure described in the text.

FIG. 7. The dispersion of a single hole in an antiferromagnetic CuO$_2$ plane measured along two directions in **k** space. The symbols represent data from the ARPES spectra from Sr$_2$CuO$_2$Cl$_2$, recorded with the indicated photon energies. The vertical error bars in the right panel indicate the errors of the fit (95% confidence interval) in determining the binding energy of the first ionization states. The **k** resolution is 0.054, 0.075, and 0.094 Å^{-1} for 16, 22, and 35 eV photon energy, respectively, which corresponds to 4.5%[6.8%], 6.3%[9.6%], and 7.8%[11.9%] of the direction $\Gamma \rightarrow (\pi,\pi)[\Gamma \rightarrow (\pi,0)]$. The lines indicate the results of the calculations employing a variational ansatz using a spin polaron with small radius (for details see text). The dashed line corresponds to a calculation where the additional transfer terms t_2 and t_3 are chosen to be zero (i.e., the tJ model), while for the solid line these terms are set to $t_2/t_1 = -0.1$ and $t_3/t_1 = 0.2$ (i.e., an extended tJ model). The improved agreement to the experimental data provided by the extended tJ model, particularly along $\Gamma \rightarrow (\pi,0)$ is apparent.

be overestimated. Nevertheless, the experimentalist is faced with a number of challenges when collecting data along this direction: firstly, at several points in the Brillouin zone, there is no or only weak photointensity from the first electron-removal state. For example, near Γ the Zhang-Rice singlet has no spectral weight, because the Cu3$d_{x^2-y^2}$ and O2p_x/O2p_y orbitals cannot hybridize there,[25] in addition the matrix elements for emission along the surface normal are formally zero for a perfectly two-dimensional electronic state located in the CuO$_2$ plane. Furthermore, near $(\pi,0)$ the photoemission intensity of the first electron-removal states becomes weak as predicted by the extended tJ models and the spin and charge separation ansatz. Secondly, only perfectly aligned samples with fresh and clean surfaces excited with UV light in a well-adjusted measurement geometry will show usable photoemission data from the first electron-removal state. Lastly, as the clean, defect-free surface of Sr$_2$CuO$_2$Cl$_2$ is highly insulating, avoiding charging effects can be difficult.

In Fig. 6 we present series of ARPES spectra recorded along $\Gamma \rightarrow (\pi,0)$ taken with parallel polarization and $\Gamma \rightarrow (\pi,\pi)$ with perpendicular polarization and with photon
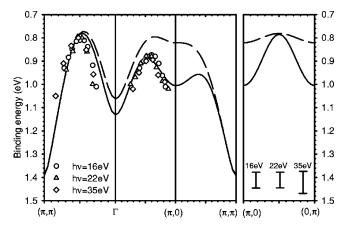
energies of 16, 22, and 35 eV — thus measuring near a peak in the photoemission intensity oscillation in each case. The position of the low energy part of the dispersive structure has been fitted using a Gaussian function while the high binding-energy background was modeled simply with the tail of another Gaussian. Although this fit is physically somewhat simplistic, it proved to be sufficient to reliably find the positions of the peak as indicated by the triangles in each plot. The absolute value on a binding-energy scale changes from one cleavage to the next and is rather arbitrary due to the insulating nature of the substance. However, the two series with 16 eV were taken during one and the same cleavage, which is the prerequisite to compare the binding-energy scales of both series. The binding-energy scales of the 22 and 35 eV data have been adjusted to that of the 16 eV data. We present a summary of the dispersion relations derived from the fits to the data in Fig. 7.

We repeat here that we observe no evidence for a photon-energy dependence of the dispersion relation of the first ionization states, as is consistent with the arguments regarding the spectral function given in the Introduction. The dispersion of the first electron-removal states along $\Gamma \rightarrow (\pi,\pi)$ agrees with the previous results having a parabolic shape with its minimum binding energy at $(\pi/2,\pi/2)$. Along $\Gamma \rightarrow (\pi,0)$ we also find a parabolic dispersion, in agreement with the dispersion reported in Refs. 20, 21 and 23, but in contrast to the data given in Ref. 19. For 16 eV

photon energy, we measured 72 meV difference in the lowest binding energies of the first electron-removal state along each of the two high-symmetry directions, which is half as small as in Ref. 20. In Ref. 21, a series of spectra representing a ''maximum intensity cut'' for a photon energy 22.4 eV along a line from $(\pi/2,\pi/2)$ to $(0.67\pi,0)$ was shown, which displayed a dispersion of about 300 meV. However, as we will show, the points of maximum intensity along $\Gamma \rightarrow (\pi,0)$ do not coincide with those possessing minimum binding energy. Thus such a maximum cut will not trace the line of minimum binding energy. It turns out that this difference strongly influences the parameters in model Hamiltonians fitted to the dispersion curves.

We now go on to compare the experimental dispersion with theoretical results obtained within the extended tJ model

$$H = -\sum_{i\sigma} \sum_{l=1}^{3} t_l X_i^{\sigma 0} X_{i+l}^{0\sigma} + J \sum_{\langle i,m \rangle} \mathbf{S}_i \cdot \mathbf{S}_m, \qquad (3)$$

with the additional hopping terms to second (t_2) and third (t_3) neighbors now added besides the dominating nearest neighbor hopping $t = t_1$. The Hamiltonian is written in terms of Hubbard operators $X_i^{\sigma 0} = c_{i\sigma}^{\dagger}(1 - n_{i-\sigma})$ where $\sigma = \pm 1$ is the spin index. The values of the hopping terms are determined by mapping the more realistic Emery model with parameters derived from a constrained density-functional calculation[39] to its low binding-energy part by means of the cell-perturbation method. This procedure gives $t_2/t_1 = -0.08$ and $t_3/t_1 = -0.15$. The theoretical dispersion relation shown in Fig. 7 is calculated using a variational method involving a spin polaron of small radius.[40] There are also related works which lead to similar dispersions.[41]

It has been shown in exact diagonalisation studies of small clusters[42] that the dispersive bandwidth scales with the single parameter, J, whereas the form of the dispersion curve is fixed by the ratios t_2/t_1 and t_3/t_1. Therefore we use the variational ansatz for $J = t_1$ and then we scale the bandwidth in Fig. 7 with a factor $J = 0.22$ eV. The excellent agreement between the results from the extended tJ model and experiment is evident. For reference, we also show the dispersion relation without additional hopping terms ($t_2 = t_3 = 0$, scaling factor $J = 0.28$ eV), which shows a much too small energy difference between the lowest binding energies of the first electron-removal states along $\Gamma \rightarrow (\pi,0)$ and $\Gamma \rightarrow (\pi,\pi)$ to obtain good agreement with the experimental spectra.

In the context of the high temperature superconductors, it is interesting to note that studies of the extended tJ model[43] indicate that upon increasing the hole doping a non-rigid band behavior is observed for the states near $(\pi,0)$. Here we have shown that the extended tJ model provides an excellent framework for understanding the low doping limit (a single hole). The results of Ref. 43 would suggest that the same model is also capable of describing the doped HTSC, with their flat bands just below E_F around $(\pi,0)$.

Another important prediction from model Hamiltonians is the evolution of the spectral weight along certain directions in the Brillouin zone. Here we map this evolution and dis-
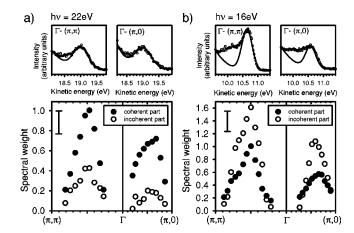

FIG. 8. The coherent and incoherent part of the spectral weight of the first electron-removal states determined from the data shown in Fig. 6 for (a) 22 eV and (b) 16 eV photon energy following the procedure used by Leung *et al.* [Phys. Rev. B **56**, 6320 (1997)]. The upper part in each case shows a representative result of the fit. In the lower part of the figure, the weight of the coherent (filled circles) and the incoherent (open circles) intensity, normalized to the coherent spectral weight at $(\pi/2,\pi/2)$, is shown. The vertical bars indicate the error of the least squares fit to the ARPES intensity (95% confidence interval).

tinguish between the coherent and incoherent parts of the first electron-removal states following the procedure proposed in Ref. 44, in which the contribution from the main valence band tail was first subtracted from the spectra. The photoemission intensity was then defined as the coherent spectral weight and fitted using a Gaussian. The ARPES intensity which is neither part of the valence band tail nor in the Gaussian is then taken to be a measure of the incoherent part of the first electron-removal state spectral function (see Ref. 44). In our case, we have used a Lorentzian broadened by the experimental resolution (i.e., a Voigt profile) to fit the lowest binding energy intensity (the coherent part). Of course, this procedure is not physically rigorous, but does offer a rough estimation of the possible split between the coherent and incoherent spectral weight.

In Fig. 8, the momentum distributions of the two parts of the ARPES spectra are shown for 16 eV and 22 eV excitation energy. Note that the overall shape of these distributions is independent of the photon energy. Along $\Gamma \rightarrow (\pi,\pi)$ both the coherent and incoherent parts of the first electron-removal states are symmetric around $(\pi/2,\pi/2)$ at which point they both reach their maximum weight. In the $\Gamma \rightarrow (\pi,0)$ direction, we observe a steady increase in spectral weight of both components up to $(0.7\pi,0)$ after which point it drops fast. One can find signs of a qualitatively similar behavior in ARPES data from other groups[19–21,23,38] and for measurements on the related substance $Ca_2CuO_2Cl_2$ (Ref. 22), although the coherent and incoherent spectral weights were not analyzed in these studies. Note that along $\Gamma \rightarrow (\pi,0)$ the minimum binding energy of the low binding-energy feature and the maximum of the coherent intensity do not coincide at the same **k** point. In calculations using extensions of the tJ model this behavior was predicted[14,45] and can now be considered as experimentally verified.

Within the simple fit procedure we can give these quantities some numbers: the ratio of the coherent to incoherent spectral weight for the two locations in **k** space is 0.6 $[(\pi/2,\pi/2)]$ and 0.5 $[(0.7\pi,0)]$ for 16 eV photon energy and 2.4 $[(\pi/2,\pi/2)]$ and 3.8 $[(0.7\pi,0)]$ for 22 eV photon energy. It is important to realize that we observe here an extremely strong apparent dependence of the *ratio* between the coherent and incoherent spectral weight upon the photon energy. To discuss the physical significance of this, we rewrite Eq. (2) as

$$S(\mathbf{k},E) = -\frac{1}{\pi} \text{Im} \left\langle i \left| c_{\mathbf{k}} \left(\frac{1}{E - E(\mathbf{k}) - \Sigma} + G_{\text{inc}} \right) c_{\mathbf{k}}^{\dagger} \right| i \right\rangle, \quad (4)$$

in order to separate the coherent from the incoherent spectral weight (Σ is the self-energy of the quasiparticle). Plugging this into Eq. (1), it is immediately clear that in taking the intensity *ratio* of the coherent and the incoherent weight, the matrix element cancels out. Thus, within this picture, this intensity ratio (a number) is then determined by the spectral function $S(\mathbf{k},E)$ alone and should not depend on the excitation energy. The form of the spectra themselves remain, of course, affected by matrix elements as can be seen in Fig. 8 and as pointed out in Ref. 23.

Our observation that the ratio does appear to depend on $h\nu$ leads then to the following possible conclusions. (i) The fit procedure used is too simple and therefore does not correctly quantify, however roughly, the coherent and incoherent parts of the spectral function. (ii) There are significant extrinsic contributions to the photoemission signal in this binding energy region. These could be the result of an energetic shift of spectral weight due to inelastic losses,[46] which could be sensitively dependent on the photoelectron kinetic energy, as are the data from electron energy loss spectroscopy in reflection of $Sr_2CuO_2Cl_2$ (Ref. 47). (iii) the photoemission intensity between the main valence band edge and the chemical potential is not derived from the spectral weight (coherent + incoherent) resulting from a *single* electronic state — i.e., there is spectral weight from an additional, different electronic state in this energy region.

The fit procedure, as we have discussed above, *is* simplistic — however the coherent-incoherent intensity ratios vary by a factor of more than four between the two photon energies. The third possible conclusion — that there has to be spectral weight from more than one state in this energy region could have important implications. We can rule out a significant contribution from secondary electrons for the relatively high kinetic energies dealt with here. Intensity from surface states is unlikely, as XPD data[48] shows that the cleavage surface of $Sr_2CuO_2Cl_2$ is terminated within the SrCl units, which are essentially ionic and therefore do not support electronic states close to the chemical potential. In addition, our LEED investigations also gave no evidence for a reconstruction of this termination layer. Spin-resolved resonant photoemission of CuO (Ref. 10) has shown intensity due to triplet states within 1 eV of the Zhang-Rice singlet, although those states would be expected to have the same photon-energy dependence as the singlet in our experiment.

If there was an additional, different state in this energy region, this would lead to a complicated **k**- and $h\nu$-dependent overlap between the intensity of this state and the higher binding energy components attributed up till now to incoherent weight from the Zhang-Rice singlet. While this would not be expected to have a large impact on the observed dispersion relation for the Zhang-Rice singlet (which is, after all, a quantity derived from the spectral structure at lowest binding energies for each **k** point), it could, however, lead to the observed photon-energy dependence of the ratio between the low binding-energy ("coherent") and higher binding-energy ("incoherent") parts of the photoemission spectra.

V. SUMMARY

In conclusion, we have presented a detailed ARPES study of the low binding-energy occupied electronic structure of $Sr_2CuO_2Cl_2$, which corresponds to an investigation of the first electron-removal states of an undoped CuO_2 plane. Our experiments, and the comparison of their results with theoretical models, have revealed the following main points.

(1) The photoemission signal of the first electron-removal states at both $(\pi/2,\pi/2)$ and $(0.7\pi,0)$ exhibits a marked photon-energy dependence. The intensity profile shows strong oscillations with maxima near 16, 25, 35, and 49 eV, corresponding to final state crystal momenta $k_\perp = 0.82$, 1.63, 2.40, and 3.12 $Å^{-1}$. This strong photon-energy dependence has complicated comparisons between data in the literature from different groups as regards both the spectral weight and spectral form of the first electron-removal states in these systems. We attribute the oscillation of photoemission intensity (which has a period in $k_\perp$ of ca. 0.75 $Å^{-1}$) to the diffraction of the photoelectron wave on the periodic c-axis separation of the CuO_2 planes of 8.2 Å.

(2) Along the high-symmetry directions $\Gamma \rightarrow (\pi,\pi)$ and $\Gamma \rightarrow (\pi,0)$ the first electron-removal states shows a strong polarization dependence. This can be linked to the strongly polarization-dependent matrix element, which in turn allows the determination of the symmetry of the first electron-removal state itself. For both high-symmetry directions we observe a polarization dependence in keeping with that expected for a Zhang-Rice singlet state in the framework of either a three-band or one-band model Hamiltonian.

(3) Our data show that the dispersion of the first electron-removal states along both high symmetry directions $[\Gamma \rightarrow (\pi,\pi)$ and $\Gamma \rightarrow (\pi,0)]$ is paraboliclike and independent of the excitation energy. This, and the rather large difference in lowest binding energy of the first electron-removal state along these directions, shows the validity of the extended tJ model for describing the disperion relation of a single hole in an antiferromagnetic CuO_2 plane. Thus, the inclusion of second (t_2) and third (t_3) neighbor hopping terms with realistic values of $t_2 = -0.08$ and $t_3 = 0.15$ in units of the next neighbor hopping $t = t_1$ are required.

(4) Upon application of a simple fit procedure, we infer the momentum distribution of the spectral weight of the coherent and incoherent part of the first electron-removal state to have its maximum along $\Gamma \rightarrow (\pi,\pi)$ at $(\pi/2,\pi/2)$ being

symmetrically suppressed away from this point. Along $\Gamma \rightarrow (\pi,0)$ the spectral weights of both parts reach their maximum at $(0.7\pi,0)$ and then drop fast. The ratio between the coherent and incoherent spectral weight is strongly photon-energy dependent, which, at first sight would appear to violate the physics of the spectral function. There are different possible explanations for this including (i) the necessity for a more sophisticated framework in which to analyze the weight of the coherent and incoherent contributions to the spectral weight, (ii) significant ($h\nu$-dependent) intensity due to extrinsic processes, and (iii) intensity in this energy region due to intrinsic electronic states *other* than the Zhang-Rice singlet.

[1] P. Aebi, J. Osterwalder, P. Schwaller, L. Schlapbach, M. Shimoda, T. Mochiku, and K. Kadowaki, Phys. Rev. Lett. **72**, 2757 (1994).

[2] Z.-X. Shen, W. E. Spicer, D. M. King, D. S. Dessau, and B. O. Wells, Science **267**, 343 (1995).

[3] L. L. Miller, X. L. Wang, S. X. Wang, C. Stassis, D. C. Johnston, J. Faber, Jr., and C.-K. Loong, Phys. Rev. B **41**, 1921 (1990).

[4] T. Sowa, M. Haritani, and K. Miyauchi, J. Solid State Chem. **84**, 178 (1990).

[5] Z. Hiroi, N. Kobayashi, and M. Takano, Nature (London) **371**, 139 (1994); M. Al-Mamouri, P. P. Edwards, C. Greaves, and M. Slaski, *ibid.* **369**, 382 (1994); Y. Zenitani, K. Inari, S. Sahoda, M. Uehara, J. Akimitsu, N. Kubota, and M. Ayabe, Physica C **248**, 167 (1995).

[6] D. Vaknin, S. K. Sinha, C. Stassis, L. L. Miller, and D. C. Johnston, Phys. Rev. B **41**, 1926 (1990).

[7] F. C. Zhang and T. M. Rice, Phys. Rev. B **37**, 3759 (1988).

[8] H. Eskes, L. H. Tjeng, and G. A. Sawatzky, Phys. Rev. B **41**, 288 (1990).

[9] Throughout this paper we strictly differentiate between the term first electron-removal state, which is a real object, and the Zhang-Rice singlet state, which is rather a theoretical construct to describe the first electron-removal state.

[10] L. H. Tjeng, B. Sinkovic, N. B. Brookes, J. B. Goedkoop, R. Hesper, E. Pellegrin, F. M. F. de Groot, S. Altieri, S. L. Hulbert, E. Shekel, and G. A. Sawatzky, Phys. Rev. Lett. **78**, 1126 (1997).

[11] A. Nazarenko, K. J. E. Vos, S. Haas, E. Dagotto, and R. J. Gooding, J. Supercond. **8**, 671 (1995); F. Mila, Phys. Rev. B **38**, 11 358 (1988); G. Dopf, A. Muramatsu, and W. Hanke, Phys. Rev. Lett. **68**, 353 (1992).

[12] M. S. Hybertsen, E. B. Stechel, M. Schlüter, and D. R. Jennison, Phys. Rev. B **41**, 11 068 (1990); L. F. Feiner, J. H. Jefferson, and R. Raimondi, *ibid.* **53**, 8751 (1996); N. Bullut, D. J. Scalapino, and S. R. White, *ibid.* **50**, 7215 (1994); E. Dagotto, F. Ortolani, and D. Scalapino, *ibid.* **46**, 3183 (1992).

[13] H. Eskes and A. M. Oleś, Phys. Rev. Lett. **73**, 1279 (1994); H. Eskes, A. M. Oleś, M. B. J. Meinders, and W. Stephan, Phys. Rev. B **50**, 17 980 (1994).

[14] H. Eskes and R. Eder, Phys. Rev. B **54**, 14 226 (1996).

[15] V. Yu. Yushankhai, V. S. Oudovenko, and R. Hayn, Phys. Rev. B **55**, 15 562 (1997).

[16] R. B. Laughlin, J. Phys. Chem. Solids **56**, 1627 (1995).

[17] R. B. Laughlin, Phys. Rev. Lett. **79**, 1726 (1997).

[18] S. Meixner, W. Hanke, E. Demler, and S.-C. Zhang, Phys. Rev. Lett. **79**, 4902 (1997); R. Eder, W. Hanke, and S.-C. Zhang, Phys. Rev. B **57**, 13 781 (1998).

[19] B. O. Wells, Z.-X. Shen, A. Matsuura, D. M. King, M. A. Kastner, M. Greven, and R. J. Birgeneau, Phys. Rev. Lett. **74**, 964 (1995).

[20] S. LaRosa, I. Vobornik, F. Zwick, H. Berger, M. Grioni, G. Margaritondo, R. J. Kelley, M. Onellion, and A. Chubukov, Phys. Rev. B **56**, R525 (1997). In this reference, conflicting statements are made as regards the polarization geometry for which the maximal intensity along $\Gamma \rightarrow (\pi,0)$ is observed. The correct situation for maximal intensity is that corresponding to ''parallel'' as used here [M. Grioni (private communication)].

[21] C. Kim, P. J. White, Z.-X. Shen, T. Tohyama, Y. Shibata, S. Maekawa, B. O. Wells, Y. J. Kim, R. J. Birgeneau, and M. A. Kastner, Phys. Rev. Lett. **80**, 4245 (1998).

[22] F. Ronning, C. Kim, D. L. Feng, D. S. Marshall, A. G. Loeser, L. L. Miller, J. N. Eckstein, I. Bozovic, and Z.-X. Shen, Science **282**, 2067 (1998).

[23] S. Haffner, C. G. Olson, L. L. Miller, and D. W. Lynch, Phys. Rev. B **61**, 14 378 (2000).

[24] Y.-D. Chuang, A. D. Gromko, D. S. Dessau, Y. Aiura, Y. Yamaguchi, K. Oka, A. J. Arko, J. Joyce, H. Eisaki, S. E. Uchida, K. Nakamura, and Y. Ando, Phys. Rev. Lett. **83**, 3717 (1999); H. M. Fretwell, A. Kaminski, J. Mesot, J. C. Campuzano, M. R. Norman, M. Randeria, T. Sato, R. Gatt, T. Takahashi, and K. Kadowaki, *ibid.* **84**, 4449 (2000); S. V. Borisenko, M. S. Golden, S. Legner, T. Pichler, C. Dürr, M. Knupfer, J. Fink, G. Yang, S. Abell, and H. Berger, *ibid.* **84**, 4453 (2000); D. L. Feng, W. J. Zheng, K. M. Shen, D. H. Lu, F. Ronning, J.-I. Shimoyama, K. Kishio, G. Gu, D. Van der Marel, and Z.-X. Shen, cond-mat/9908056 (unpublished); S. Legner, S. V. Borisenko, C. Dürr, T. Pichler, M. Knupfer, M. S. Golden, J. Fink, G. Yang, S. Abell, H. Berger, R. Mueller, C. Janowitz, and G. Reichardt, Phys. Rev. B **62**, 154 (2000).

[25] J. J. M. Pothuizen, R. Eder, N. T. Hien, M. Matoba, A. A. Menovsky, and G. A. Sawatzky, Phys. Rev. Lett. **78**, 717 (1997).

[26] R. Hayn, H. Rosner, V. Yu. Yushankhai, S. Haffner, C. Dürr, M. Knupfer, G. Krabbes, M. S. Golden, J. Fink, H. Eschrig, D. J. Singh, N. T. Hien, A. A. Menovsky, C. Jung, and G. Reichardt, Phys. Rev. B **60**, 645 (1999).

[27] M. Greven, R. J. Birgeneau, Y. Endoh, M. A. Kastner, B. Keimer, M. Matsuda, G. Shirane, and T. R. Thurston, Phys. Rev. Lett. **72**, 1096 (1994).

[28] We refer to the notation in Ref. 19 where $\Gamma=(0,0)$ means the center and $(\pm\pi,\pm\pi)$ means the corners of the two-dimensional Brillouin zone of the square-planar CuO_2 plane given in units $1/a$ where $a=3.967$ Å is the lattice constant of $Sr_2CuO_2Cl_2$ (Ref. 3).

[29] R. Courths and S. Hüfner, Phys. Rep. **112**, 53 (1984).

[30] Y. B. Xu, M. Q. Tan, and U. Becker, Phys. Rev. Lett. **76**, 3538 (1996).

[31] J. G. Tobin, C. G. Olson, C. Gu, J. Z. Liu, F. R. Solal, M. J. Fluss, R. H. Howell, J. C. O'Brian, H. B. Radousky, and P. A. Sterne, Phys. Rev. B **45**, 5563 (1992).

[32] A. Bansil and M. Lindroos, Phys. Rev. Lett. **83**, 5154 (1999).

[33] G. W. Gobeli, F. G. Allen, and E. O. Kane, Phys. Rev. Lett. **12**, 94 (1964); E. Dietz, H. Becker, and U. Gerhardt, *ibid.* **36**, 1397 (1976); J. Hermanson, Solid State Commun. **22**, 9 (1997).

[34] S. A. Trugman, Phys. Rev. Lett. **65**, 500 (1990).

[35] Z. Liu and E. Manousakis, Phys. Rev. B **45**, 2425 (1992).

[36] E. Dagotto and A. Nazarenko, Phys. Rev. Lett. **73**, 728 (1994).

[37] A. Moreo, S. Haas, A. W. Sandvik, and E. Dagotto, Phys. Rev. B **51**, 12 045 (1995).

[38] S. Haffner, D. M. Brammeier, C. G. Olson, L. L. Miller, and D. W. Lynch, cond-mat/0006366 (unpublished).

[39] M. S. Hybertsen, E. B. Stechel, M. Schlüter, and D. R. Jennison, Phys. Rev. B **41**, 11 068 (1990).

[40] R. Hayn, A. F. Barabanov, and J. Schulenburg, Z. Phys. B: Condens. Matter **102**, 359 (1997).

[41] A. Nazarenko, K. J. E. Vos, S. Haas, E. Dagotto, and R. J. Gooding, Phys. Rev. B **51**, 8676 (1995); V. I. Belinicher, A. L. Chernyshev, and V. A. Shubin, *ibid.* **54**, 14 914 (1996); T. Xiang and J. M. Wheatley, *ibid.* **54**, R12 653 (1996); F. Lema and A. A. Aligia, *ibid.* **55**, 14 092 (1997); J. Eroles, C. D. Batista, and A. A. Aligia, *ibid.* **59**, 14 092 (1999).

[42] E. Dagotto, R. Joynt, A. Moreo, S. Bacci, and E. Gagliano, Phys. Rev. B **41**, 9049 (1990).

[43] R. Eder, Y. Oths, and G. A. Sawatzky, Phys. Rev. B **55**, 3414 (1997).

[44] P. W. Leung, B. O. Wells, and R. J. Gooding, Phys. Rev. B **56**, 6320 (1997).

[45] B. Kyung and R. A. Ferrell, Phys. Rev. B **54**, 10 125 (1996).

[46] R. Joynt, Science **284**, 777 (1999).

[47] J. J. M. Pothuizen, Ph.D. thesis, University of Groningen, 1998.

[48] T. Böske, O. Knauff, R. Neudert, M. Kielwein, M. Knupfer, M. S. Golden, and J. Fink, Phys. Rev. B **56**, 3438 (1997).